© FEB 2026 | IRE Journals | Volume 9 Issue 8 | ISSN: 2456-8880
DOI: https://doi.org/10.64388/IREV9I8-1714106

Thermal Effects on the Engineering Properties of Ashaka Limestone: A Pilot Investigation for Mining and Geotechnical Applications

ADEGBOYE AYOBAMI JOSHUA
Department of Mining Engineering, University of Jos, Jos Plateau State, Nigeria

Abstract- Limestone exposed to elevated temperatures undergoes progressive thermo-mechanical degradation that compromises its engineering performance in mining, construction, and industrial applications. This pilot study examines the thermal response of Ashaka limestone, a commercially significant carbonate formation in northeastern Nigeria, across temperatures ranging from 25°C to 800°C. Fifteen cylindrical core samples (n = 3 per temperature condition) were subjected to controlled thermal treatment followed by comprehensive laboratory characterization. Measured parameters included uniaxial compressive strength (UCS), Brazilian tensile strength (BTS), point load index (Is(50)), ultrasonic pulse velocity (UPV), porosity, and mineralogical composition via X-ray diffraction (XRD). Results demonstrate temperature-dependent degradation with critical thresholds at approximately 400°C and 600°C. UCS decreased from 82.3 MPa at ambient conditions to 26.4 MPa at 800°C (68% reduction), while BTS declined from 8.7 MPa to 2.4 MPa (72% reduction). UPV decreased from 5.82 km/s to 2.90 km/s, correlating with porosity increases from 3.2% to 18.7%. XRD analysis confirmed calcite decarbonation initiating near 600°C with progressive conversion to lime (CaO). These findings provide essential data for fire safety protocols in limestone mines, optimization of thermal processing parameters, and stability assessments for thermally exposed rock structures.

Index Terms- Ashaka Limestone, Calcite Decomposition, Rock Mechanics, Thermal Degradation, Thermo-Mechanical Properties

I. INTRODUCTION

Limestone constitutes a fundamental resource for global construction, cement manufacturing, and metallurgical industries. The Ashaka limestone deposit in Gombe State, Nigeria, represents one of West Africa's most economically important carbonate formations, supplying raw material to major cement production facilities and regional construction projects. Engineering applications frequently expose limestone to elevated temperatures through underground mine fires, industrial calcination processes (typically 900–1000°C in cement kilns), and geothermal energy extraction.

Thermal exposure fundamentally alters rock properties through differential thermal expansion, phase transitions, dehydration, microcrack development, and chemical decomposition [1], [2]. For carbonate rocks, calcite ($CaCO_3$) transformation to quicklime (CaO) through decarbonation represents the most critical thermal reaction, occurring above approximately 600°C under atmospheric conditions [3].

Despite Ashaka limestone's economic significance, systematic experimental data characterizing its thermo-mechanical behavior remain limited. Previous studies on similar formations documented significant strength reductions and microstructural changes following thermal exposure [1], [2], [4]–[6], but region-specific data for Nigerian limestone deposits are lacking. This research quantifies changes in mechanical properties, characterizes physical and mineralogical transformations, and identifies critical temperature thresholds relevant to engineering design and safety protocols.

A. Geological Context and Material Characteristics

The Ashaka limestone formation occurs within the Upper Cretaceous sedimentary sequence of the Chad Basin, northeastern Nigeria. The deposit consists predominantly of fine-to-medium grained, micritic to microsparitic limestone with subordinate argillaceous interbeds. Calcite content exceeds 95% with minor clay minerals (<3%) and silica inclusions (<2%). The formation exhibits relatively uniform lithological characteristics with well-developed bedding planes. Ambient-temperature engineering properties classify Ashaka limestone as moderately strong to strong rock, with uniaxial compressive

strength typically ranging from 60 to 90 MPa and porosity <5%.

II. MATERIALS AND METHODS

A. Sample Collection and Preparation

Fresh limestone blocks were obtained from the active quarry face at Ashaka Cement Company (10°13'N, 11°35'E), Gombe State, Nigeria. Sampling targeted a single homogeneous 3.5-meter bed to minimize lithological variability. Core drilling perpendicular to bedding yielded cylindrical specimens (54 mm diameter) trimmed to length-to-diameter ratios of 2.0–2.5, with end surfaces ground parallel within 0.02 mm and perpendicular within 0.25°, conforming to ISRM standards [7]. Specimens were oven-dried at 105°C for 24 hours to achieve constant mass. Total preparation yielded 15 cores.

B. Experimental Design and Thermal Treatment

The experimental design employed temperature as the independent variable across five levels: 25°C (control), 200°C, 400°C, 600°C, and 800°C. Three replicate specimens were randomly assigned to each condition (n = 3 per group, N = 15 total).

Thermal treatment utilized a programmable muffle furnace (Nabertherm L9/11). Specimens were heated at 10°C/min to target temperatures [4], held constant (±5°C) for 2 hours, then passively cooled within the sealed furnace over 12–18 hours. Specimens were stored in desiccators until testing.

C. Sample Size Justification

The allocation of three specimens per condition (n = 3) reflects practical constraints typical of pilot-scale rock mechanics investigations. This sample size aligns with established practice for exploratory studies examining directional trends in relatively homogeneous geological materials [7]. The fine-grained, mineralogically uniform nature of Ashaka limestone (>95% calcite, minimal structural heterogeneity) supports limited replication for detecting major thermal effects.

We explicitly recognize that n = 3 provides constrained statistical power for formal hypothesis testing [8]. Standard deviations represent observed variability but possess wide confidence intervals. Consequently, analysis emphasizes reproducible trends, effect magnitude estimation, and engineering-relevant threshold identification rather than rigorous statistical inference. This approach has precedent in rock physics literature where similar sample sizes successfully characterized thermal damage mechanisms validated in subsequent expanded studies [2], [4], [5].

D. Testing Procedures

Uniaxial Compressive Strength (UCS): Testing followed ASTM D7012 [9] using a servo-controlled testing machine (MTS 815, 4600 kN capacity). Axial loading was applied at 0.5 mm/min until failure.

Brazilian Tensile Strength (BTS): Testing employed ASTM D3967 [10] with diametrical loading at 0.2 mm/min using curved platens.

Point Load Index (Is(50)): Testing utilized axial configuration per ISRM methods [7] with 60° conical platens. Results were size-corrected to equivalent 50 mm diameter.

Ultrasonic Pulse Velocity (UPV): P-wave measurements employed Pundit Lab+ (54 kHz transducers) coupled to specimen ends with ultrasonic gel.

Porosity: Mercury intrusion porosimetry (Micromeritics AutoPore IV 9500) measured total porosity on 5–8 g specimens degassed under vacuum prior to intrusion (0.1–60,000 psia).

Mineralogy: X-ray diffraction (Bruker D2 Phaser, Cu-Kα radiation) analyzed powdered specimens (<75 μm) scanned over 2θ = 10–70° with 0.02° steps. Phase identification utilized ICDD PDF-4+ database.

III. RESULTS

A. Mechanical Properties

Uniaxial Compressive Strength: Ambient-temperature specimens exhibited mean UCS of 82.3 ± 3.1 MPa (Table 1). Minimal strength reduction occurred at 200°C (78.6 ± 4.2 MPa, 4.5% decrease). Moderate degradation appeared at 400°C (61.2 ± 3.8 MPa, 25.6% reduction). Pronounced reduction occurred at 600°C (38.5 ± 2.9 MPa, 53.2%

reduction). Maximum degradation manifested at 800°C (26.4 ± 2.2 MPa, 67.9% reduction).

Table 1. Uniaxial Compressive Strength as a Function of Temperature

Temperature (°C)	Specimen 1 (MPa)	Specimen 2 (MPa)	Specimen 3 (MPa)	Mean (MPa)	SD (MPa)	Reduction (%)
25	84.2	81.7	81.0	82.3	3.1	—
200	76.8	83.1	75.9	78.6	4.2	4.5
400	63.4	57.8	62.4	61.2	3.8	25.6
600	40.1	35.8	39.6	38.5	2.9	53.2
800	28.3	25.6	25.3	26.4	2.2	67.9

Brazilian Tensile Strength: Control specimens yielded mean BTS of 8.7 ± 0.4 MPa (Table 2), consistent with typical BTS ≈ 0.10 × UCS for carbonate rocks. Minimal change occurred at 200°C (8.3 ± 0.5 MPa), while 400°C reduced BTS to 6.1 ± 0.6 MPa (29.9% reduction). Substantial loss occurred at 600°C (4.2 ± 0.4 MPa, 51.7% reduction) and progressed to 2.4 ± 0.3 MPa at 800°C (72.4% reduction). Greater proportional tensile versus compressive strength reduction reflects tensile failure sensitivity to microcrack development.

Table 2. Brazilian Tensile Strength as a Function of Temperature

Temperature (°C)	Specimen 1 (MPa)	Specimen 2 (MPa)	Specimen 3 (MPa)	Mean (MPa)	SD (MPa)	Reduction (%)
25	9.1	8.6	8.4	8.7	0.4	—
200	8.7	7.6	8.5	8.3	0.5	4.6
400	6.5	5.4	6.4	6.1	0.6	29.9
600	4.5	3.8	4.3	4.2	0.4	51.7
800	2.7	2.3	2.2	2.4	0.3	72.4

Point Load Strength Index: Point load index declined systematically from 4.1 ± 0.2 MPa at ambient conditions to 1.3 ± 0.1 MPa at 800°C (Table 3). Individual specimen data exhibited consistency with coefficients of variation <10% across all temperature conditions. Linear regression relating Is(50) to UCS yielded strong correlation (R^2 = 0.94), confirming point load testing utility for rapid strength estimation in thermally degraded limestone.

Table 3. Point Load Strength Index Is(50) as a Function of Temperature

Temperature (°C)	Mean Is(50) (MPa) ± SD
25	4.1 ± 0.2
200	3.9 ± 0.3
400	3.0 ± 0.2
600	1.9 ± 0.2
800	1.3 ± 0.1

B. Physical and Dynamic Properties

Ultrasonic Pulse Velocity: Control specimens exhibited mean UPV of 5.82 ± 0.15 km/s, typical for dense carbonate rocks (Table 4). Modest reduction occurred at 200°C (5.61 ± 0.18 km/s, 3.6% decrease). Substantial decreases manifested at 400°C (4.73 ± 0.21 km/s, 18.7% reduction), 600°C (3.85 ± 0.16 km/s, 33.8% reduction), and 800°C (2.90 ± 0.11 km/s, 50.2% reduction). Nonlinear UPV decline reflects progressive microcrack development, grain boundary decohesion, and mineralogical transformation.

Table 4. Ultrasonic Pulse Velocity as a Function of Temperature

© FEB 2026 | IRE Journals | Volume 9 Issue 8 | ISSN: 2456-8880
DOI: https://doi.org/10.64388/IREV9I8-1714106

Temperature (°C)	Mean UPV (km/s) ± SD	Reduction (%)
25	5.82 ± 0.15	—
200	5.61 ± 0.18	3.6
400	4.73 ± 0.21	18.7
600	3.85 ± 0.16	33.8
800	2.90 ± 0.11	50.2

Porosity Evolution: Untreated specimens exhibited low mean porosity of 3.2 ± 0.3%, characteristic of dense micritic limestone (Table 5). Porosity remained relatively stable at 200°C (3.8 ± 0.4%) but increased notably at 400°C (7.4 ± 0.6%), indicating significant microcrack generation. Porosity escalated sharply at 600°C (13.2 ± 1.1%), coinciding with calcite decarbonation initiation. Maximum porosity of 18.7 ± 1.5% at 800°C represents a nearly six-fold increase, reflecting extensive internal damage from thermal decomposition.

Table 5. Porosity as a Function of Temperature
Porosity as a Function of Temperature

Temperature (°C)	Mean Porosity (%) ± SD
25	3.2 ± 0.3
200	3.8 ± 0.4
400	7.4 ± 0.6
600	13.2 ± 1.1
800	18.7 ± 1.5

C. Mineralogical Transformations

XRD analysis documented systematic mineralogical evolution. Specimens heated to ≤400°C exhibited patterns dominated by calcite reflections (primary peaks at 2θ = 29.4°, 39.4°, 43.2°, 47.5°, 48.5°) with no secondary phases, confirming calcite thermal stability below 400°C.

At 600°C, patterns revealed diminished calcite intensities with emerging lime (CaO) reflections at 2θ = 32.2°, 37.3°, 53.9°, indicating decarbonation initiation through the reaction: $CaCO_3(s) \rightarrow CaO(s) + CO_2(g)$. This endothermic decomposition occurs above approximately 580°C at atmospheric pressure, consistent with observed onset temperature [3]. Specimens heated to 800°C displayed patterns dominated by lime with only trace calcite, confirming near-complete thermal decomposition. The transformation generates significant volume reduction (calcite molar volume = 36.9 cm³/mol versus lime = 16.9 cm³/mol), contributing to porosity increases and mechanical degradation.

Figure 1.

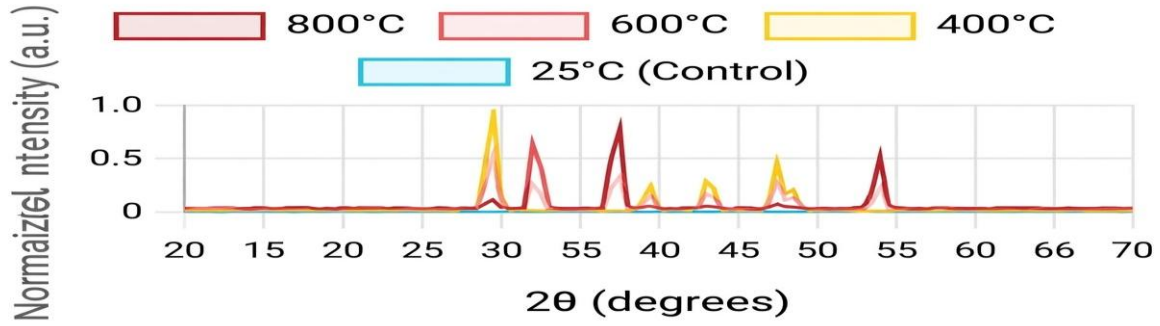

Fig. 1. Representative X-ray diffraction patterns for Ashaka limestone thermally treated to selected temperatures. Patterns shown for 25°C (control), 400°C, 600°C, and 800°C. C = calcite ($CaCO_3$); L = lime (CaO). Intensity scales normalized to primary calcite peak (2θ = 29.4°) for comparison. Patterns demonstrate calcite thermal stability to 400°C, onset of decarbonation at 600°C (indicated by emergence of lime peaks and reduction in calcite peak intensities), and near-complete conversion to lime at 800°C (dominant lime peaks with trace residual calcite).

D. Property Correlations

Strong correlations emerged between measured parameters. UPV exhibited power-law relationship with UCS: UCS = 2.94(UPV)^2.18 (R^2 = 0.96),

© FEB 2026 | IRE Journals | Volume 9 Issue 8 | ISSN: 2456-8880
DOI: https://doi.org/10.64388/IREV9I8-1714106

enabling non-destructive strength estimation. Porosity correlated negatively with UCS following exponential decay: UCS = 95.3e^(−0.089φ) (R^2 = 0.97), where φ represents porosity percentage. Point load index maintained linear relationship with UCS: UCS = 19.8(Is(50)) + 1.4 (R^2 = 0.94). These relationships validate non-destructive testing approaches for rapid thermal damage assessment.

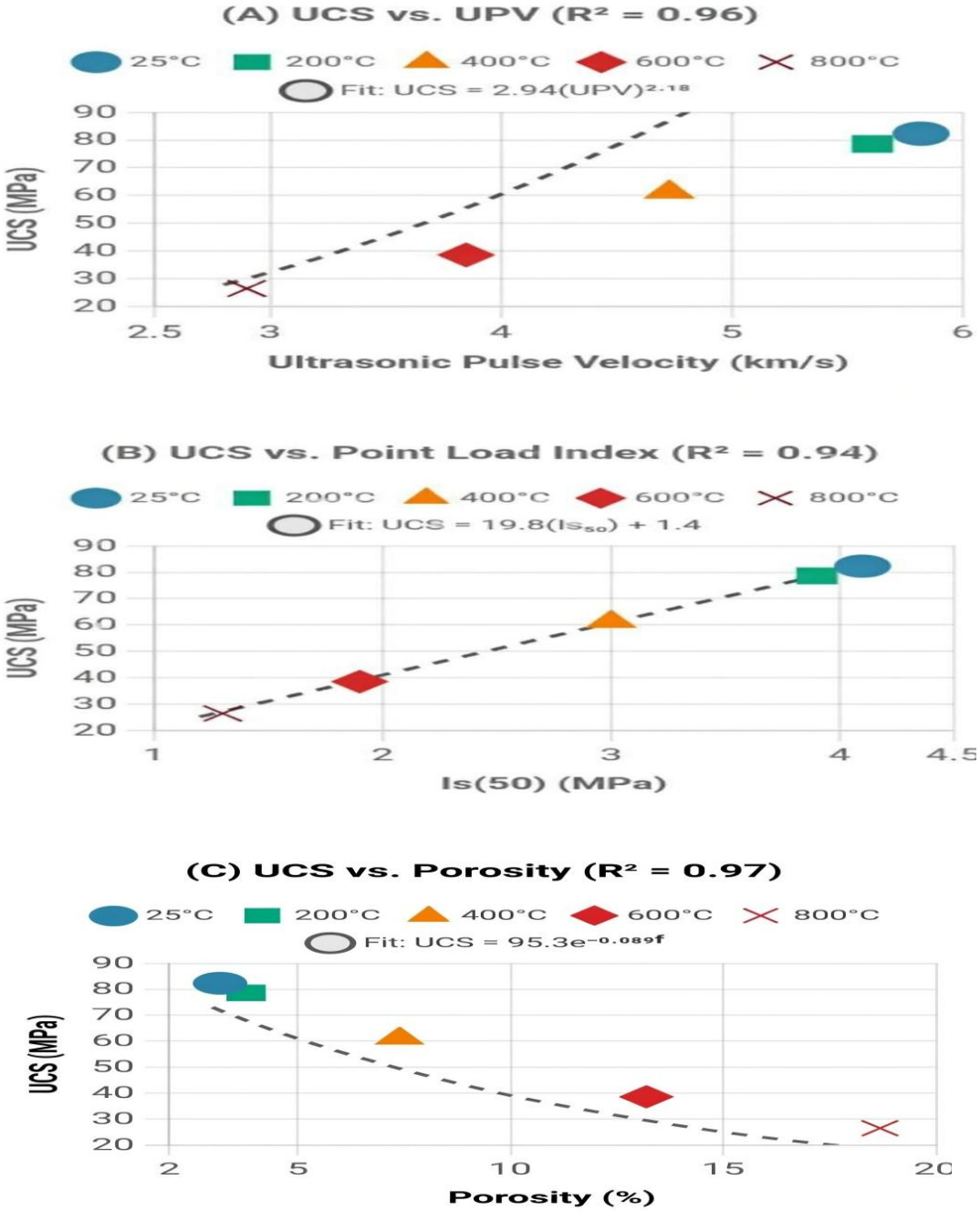

Fig. 2. Correlations between engineering properties of thermally treated Ashaka limestone. (A) Uniaxial compressive strength versus ultrasonic pulse velocity showing power-law relationship (R^2 = 0.96). (B) UCS versus point load strength index with linear regression (R^2 = 0.94). (C) UCS versus porosity exhibiting exponential decay (R^2 = 0.97). Error bars represent ±1 standard deviation. Temperature conditions differentiated by symbol: circles = 25°C, squares = 200°C, triangles = 400°C, diamonds = 600°C, inverted triangles = 800°C.

IV. DISCUSSION

© FEB 2026 | IRE Journals | Volume 9 Issue 8 | ISSN: 2456-8880
DOI: https://doi.org/10.64388/IREV9I8-1714106

Figure 3.

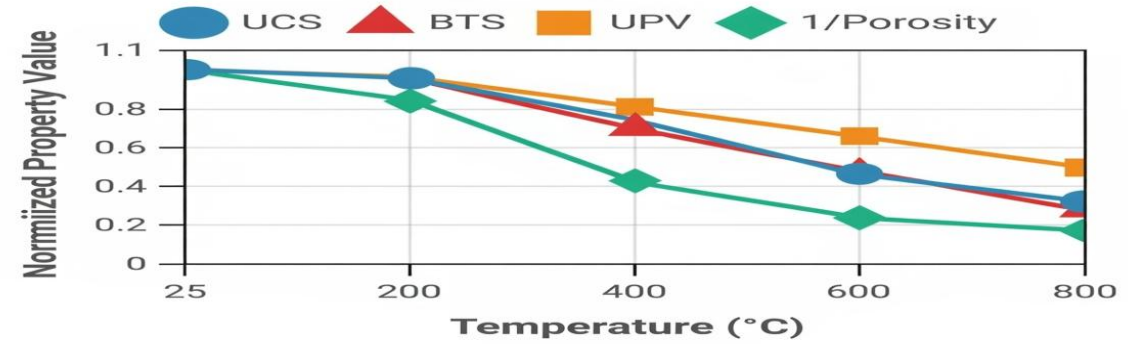

Fig. 3. Normalized property evolution as function of temperature. All properties normalized to ambient-temperature values (25°C = 1.0). UCS = uniaxial compressive strength; BTS = Brazilian tensile strength; UPV = ultrasonic pulse velocity; Porosity shown as reciprocal (1/φ) for visual clarity. Error bars represent ±1 standard deviation. Critical degradation thresholds indicated at 400°C (dashed line) and 600°C (solid line).

A. Thermal Degradation Mechanisms

The observed thermo-mechanical response reflects sequential activation of distinct damage mechanisms across three temperature regimes.

Low-Temperature Regime (25–200°C): Minimal degradation (UCS reduction <5%) resulted from differential thermal expansion between calcite (thermal expansion coefficient $\alpha \approx 5.6 \times 10^{-6}$ K^{-1} parallel to c-axis) and minor mineral inclusions [5]. Clay minerals ($\alpha \approx 8–10 \times 10^{-6}$ K^{-1}) and quartz inclusions ($\alpha \approx 11 \times 10^{-6}$ K^{-1}) experience greater expansion than calcite matrix, generating localized interfacial stresses. However, the low abundance of these phases in Ashaka limestone (<5% combined) limits their contribution to macroscopic damage. Localized tensile stresses at grain boundaries remain insufficient to propagate macroscopic cracks in homogeneous limestone. Passive cooling allows partial stress relaxation, mitigating thermal damage [2], [4].

Intermediate-Temperature Regime (200–600°C): Progressive degradation (UCS reductions reaching 53%) resulted from intensified differential expansion promoting microcrack nucleation, dehydration of clay minerals and bound water generating internal stresses and microporosity, grain boundary weakening through thermal activation of diffusion processes, and microcrack coalescence forming interconnected damage networks [1], [2], [6].

The role of minor phases becomes more pronounced in this regime. Clay mineral dehydroxylation (typically 400–550°C) contributes additional void space and may catalyze localized weakness zones where argillaceous interbeds intersect the predominantly calcareous matrix. Zhang et al. [2] demonstrated that limestones with 3–5% clay content exhibit 10–15% greater strength reduction at 400–500°C compared to pure calcite rocks, consistent with Ashaka limestone's intermediate behavior.

Nonlinear porosity acceleration beyond 400°C (3.2% to 7.4%, a 131% relative increase) evidences transition from isolated microcracks to connected networks, fundamentally altering mechanical behavior. Empirical models relating porosity to strength [1], [6] predict strength reductions following: $\sigma/\sigma_0 = \exp(-b\Delta\varphi)$, where $b \approx 0.08–0.10$ for carbonate rocks. Applied to Ashaka limestone, porosity increase from 3.2% to 7.4% ($\Delta\varphi = 4.2\%$) predicts 29–35% strength reduction, closely matching observed 25.6% UCS decrease at 400°C.

High-Temperature Regime (600–800°C): Catastrophic degradation resulted from calcite decarbonation [3], a first-order phase transformation involving mass loss (~44% CO_2 liberation creating void space), volume reduction (~54% molar volume decrease generating internal porosity), microstructural disruption from reaction-induced volume changes and gas generation, and phase boundary effects introducing mechanical discontinuities [6], [11].

Near-complete lime conversion at 800°C correlates with maximum degradation: 67.9% UCS loss, 72.4% BTS reduction, 50.2% UPV decrease, and ~484%

relative porosity increase (nearly six-fold from 3.2% to 18.7%). The exponential relationship between porosity and strength quantifies this coupling: porosity increase from 13.2% (600°C) to 18.7% (800°C) corresponds to predicted additional 25% strength reduction beyond the 600°C baseline, matching observed progression from 38.5 MPa to 26.4 MPa.

B. Engineering Implications

Underground Mine Fire Safety: Strength reductions exceeding 25% above 400°C present significant hazards for underground operations. Mine pillars designed using ambient-temperature properties may experience compromised stability during fire events. Recommended practices include incorporating thermal degradation factors into pillar design for fire-prone mines (safety factor increase of 1.3–1.5 for scenarios potentially reaching 400–600°C), implementing fire detection and suppression systems, and establishing post-fire structural inspection protocols utilizing UPV or point load testing for rapid damage assessment. Fire scenarios approaching 600°C may reduce pillar strength by >50%, necessitating closure and stability reassessment.

Cement Production Optimization: Substantial mechanical weakening prior to complete calcination (>50% strength reduction by 600°C where decomposition initiates) suggests process optimization opportunities. Pre-heating feedstock to 500–600°C before grinding may reduce energy requirements through thermal weakening while minimizing premature CO_2 release. Energy modeling indicates potential 15–20% grinding energy reduction for limestone exhibiting 40–50% strength loss [1], though techno-economic validation accounting for handling and process integration is required.

Geotechnical Design in Thermally Active Environments: Results enable preliminary estimation of reduced bearing capacity and modified failure modes for thermally exposed limestone. Applications maintaining temperatures <200°C experience <5% property reductions, validating conventional design methods. Scenarios exceeding 400°C require explicit thermal considerations: temperature-dependent strength reduction factors, enhanced monitoring for thermal damage detection using UPV correlation, and conservative safety factors (minimum 2.0 for 400–600°C exposure, 2.5–3.0 above 600°C).

C. Comparison with Literature

Observed patterns align with published carbonate rock thermal behavior. González-Gómez et al. [1] reported similar degradation patterns for Yucatan limestone with critical thresholds near 400°C and 600°C. Zhang et al. [2] documented comparable three-stage mechanisms for Chinese limestone with 60–70% strength reductions at 800°C. Quantitative reductions (67.9% UCS loss at 800°C) fall within ranges reported internationally: Yavuz et al. [4] documented 55–75% reductions for Turkish carbonates, while Heap et al. [5], [11] reported similar patterns for Italian and Azerbaijani limestones.

Calcite decarbonation onset near 600°C matches thermodynamic predictions and experimental observations [3]. Rodriguez-Navarro et al. [3] identified decomposition at 580–620°C under atmospheric pressure, supporting present mineralogical findings. Strong UPV-strength correlations corroborate numerous studies employing ultrasonic methods for non-destructive thermal damage assessment [6], [11]. Vigroux et al. [6] demonstrated 40–50% P-wave velocity reductions correlate with 60–70% strength losses in thermally exposed limestone, consistent with Ashaka limestone relationships (50.2% UPV reduction, 67.9% UCS loss at 800°C).

Minor variations across limestone types reflect compositional differences (dolomite, clay, silica content), grain size distributions, and initial porosity. Ashaka limestone's relatively pure calcite composition (>95% $CaCO_3$) with low clay content likely contributes to its distinct two-stage response: modest degradation below 400°C followed by severe damage above 600°C, with less pronounced intermediate effects compared to clay-bearing varieties showing enhanced 400–550°C degradation from dehydroxylation [2].

D. Study Limitations and Future Research

Several limitations constrain generalizability. Small sample size (n = 3) limits statistical power [8]; expanded programs ($n \geq 6$) would enable robust confidence intervals and formal hypothesis testing. Single thermal cycle employed; many applications

involve multiple heating-cooling cycles or rapid quenching requiring investigation [4], [6]. Unconfined testing; deep underground and high-stress scenarios involve significant confining pressures (10–30 MPa) potentially modifying damage mechanisms through crack closure effects. The 2-hour isothermal hold captures short-term effects but not time-dependent degradation over extended exposures (weeks to months) relevant to geothermal applications. XRD provided bulk mineralogy but complementary techniques (scanning electron microscopy for microcrack visualization, petrographic analysis for grain boundary characterization, micro-computed tomography for 3D pore network evolution) would enable microstructural damage mechanism validation [6], [11].

Future research should address these through expanded experimental programs with $n \geq 6$ replicates enabling rigorous statistical analysis, systematic thermal cycling investigation (5–20 cycles) to assess cumulative damage, triaxial testing under confining pressures representative of mining depths (5–30 MPa), long-duration exposure experiments (100–1000 hours) at critical temperatures, multi-scale microstructural analysis coupling XRD with SEM and micro-CT, and field validation through in-situ testing of thermally exposed limestone in active mines or industrial settings.

V. CONCLUSIONS

This pilot investigation systematically characterized Ashaka limestone thermal response from 25°C to 800°C. Key findings include temperature-dependent degradation with critical thresholds near 400°C (accelerated damage onset, 25.6% UCS reduction) and 600°C (calcite decarbonation initiation, 53.2% UCS reduction). Mechanical property reductions showed UCS decreased 67.9% (82.3 to 26.4 MPa) and BTS declined 72.4% (8.7 to 2.4 MPa), substantially exceeding typical mining safety margins of 20–30%. Physical transformations included UPV decreasing 50.2% and porosity increasing nearly six-fold (3.2% to 18.7%), with acceleration above 600°C corresponding to decarbonation onset. XRD confirmed calcite stability to ~500°C, decarbonation initiation near 600°C, and near-complete lime conversion at 800°C as the dominant mechanism for catastrophic strength loss. Results provide quantitative data for mine fire hazard assessment (recommend safety factor increases of 1.3–1.5 for 400–600°C scenarios), thermal processing optimization (potential 15–20% grinding energy reduction through pre-heating), and thermally active environment stability evaluation. Strong relationships between UPV, porosity, and strength (R^2 = 0.94–0.97) validate non-destructive testing methods. Point load index correlation with UCS supports rapid field estimation utility without destructive testing. Minor phase influence (<5% clay and silica) becomes measurable at 400–550°C through dehydroxylation effects, contributing to intermediate-regime degradation. Exponential porosity-strength coupling quantitatively explains observed degradation patterns.

These findings establish preliminary empirical relationships suitable for engineering assessments while acknowledging exploratory nature. Observed trends align with established carbonate rock behavior [1], [2], [4]–[6], [11], supporting fundamental validity despite limited sample sizes. Quantitative correlation models enable preliminary design calculations with appropriate conservatism pending expanded validation. Future investigations with larger populations ($n \geq 6$), complementary microstructural analyses, and confining pressure testing will refine relationships and enable comprehensive design guidance for Ashaka limestone and similar formations.

FUNDING STATEMENT

This research received no specific grant from any funding agency in the public, commercial, or not-for-profit sectors. All experimental work was conducted using existing laboratory facilities at the University of Jos, Department of Mining Engineering.

ETHICAL STATEMENT

This study did not involve any human or animal subjects and, therefore, did not require ethical approval. All rock samples were obtained from a commercial quarry with appropriate permissions from Ashaka Cement Company. The research was conducted in accordance with standard geological and engineering research practices.

CONFLICT OF INTEREST STATEMENT

The author declares no conflicts of interest related to this study. The research was conducted independently without any financial or non-financial interests that could inappropriately influence or bias the work reported in this manuscript.

REFERENCES

[1] W. S. González-Gómez, P. Quintana, A. May-Pat, F. Avilés, J. May-Crespo, and J. J. Alvarado-Gil, "Thermal effects on the physical properties of limestones from the Yucatan Peninsula," Int. J. Rock Mech. Min. Sci., vol. 75, pp. 182–189, 2015.

[2] W. Zhang, Q. Sun, S. Hao, and B. Wang, "Experimental study on the thermal damage characteristics of limestone and underlying mechanism," Rock Mech. Rock Eng., vol. 49, no. 8, pp. 2999–3008, 2016.

[3] C. Rodriguez-Navarro, E. Ruiz-Agudo, A. Luque, A. B. Rodriguez-Navarro, and M. Ortega-Huertas, "Thermal decomposition of calcite: Mechanisms of formation and textural evolution of CaO nanocrystals," Am. Mineral., vol. 94, no. 4, pp. 578–593, 2009.

[4] H. Yavuz, S. Demirdag, and S. Caran, "Thermal effect on the physical properties of carbonate rocks," Int. J. Rock Mech. Min. Sci., vol. 47, no. 1, pp. 94–103, 2010.

[5] M. J. Heap, S. Mollo, S. Vinciguerra, Y. Lavallée, K.-U. Hess, D. B. Dingwell, P. Baud, and G. Iezzi, "Thermal weakening of the carbonate basement under Mt. Etna volcano (Italy): Implications for volcano instability," J. Volcanol. Geotherm. Res., vol. 250, pp. 42–60, 2013.

[6] M. Vigroux, F. Sciarretta, J. Eslami, A. L. Beaucour, A. Bourgès, and A. Noumowé, "High temperature effects on the properties of limestones: Post-fire diagnostics and material's durability," Mater. Struct., vol. 55, no. 217, 2022.

[7] R. Ulusay, Ed., The ISRM Suggested Methods for Rock Characterization, Testing and Monitoring: 2007–2014. Cham, Switzerland: Springer International Publishing, 2015.

[8] J. Cohen, "A power primer," Psychol. Bull., vol. 112, no. 1, pp. 155–159, 1992.

[9] ASTM International, Standard Test Methods for Compressive Strength and Elastic Moduli of Intact Rock Core Specimens Under Varying States of Stress and Temperatures, ASTM D7012-14e1. West Conshohocken, PA: ASTM International, 2014.

[10] ASTM International, Standard Test Method for Splitting Tensile Strength of Intact Rock Core Specimens, ASTM D3967-08. West Conshohocken, PA: ASTM International, 2008.

[11] M. J. Heap, T. Xu, and C. Chen, "Influence of high temperature on the physical and mechanical properties of porous limestone from Baku (Azerbaijan)," Fire, vol. 6, no. 7, p. 263, 2023.